ELSEVIER

Available online at www.sciencedirect.com

SCIENCE DIRECT

Journal of Crystal Growth 251 (2003) 124–129

JOURNAL OF CRYSTAL GROWTH

www.elsevier.com/locate/jcrysgro

InGaAs composition monitoring for production MBE by in situ optical-based flux monitor (OFM)

Paul R. Pinsukanjana*, Jeremy M. Marquis, Jared Hubbard, Mehul A. Trivedi, Roger F. Dickey, Jerry M.-S. Tsai, Sam P. Kuo, Philip S. Kao, Yung-Chung Kao

Intelligent Epitaxy Technology Inc., 1250 Collins Blvd., Richardson, TX 75081, USA

Abstract

Atomic absorption optical-based flux monitor (OFM) has been implemented as a non-invasive in situ measurement tool for production MBE operation. For our setup, the optical probe beam samples the group III beam fluxes (Al, Ga, and In) by passing just in front of the substrate platen. The multi-species atomic absorption profile taken during MBE becomes a record for each epi-layer growth. For InGaAs critical layers in devices such as GaAs-based PHEMTs and InP-based HBTs, OFM is used to monitor the In mole fraction. Data sets of $In_xGa_{1-x}As$ composition measured by OFM are taken from two different sizes of multi-wafer reactors and compared to the results from X-ray diffraction measurements. The standard deviation of the difference between the two measurement techniques for $x = 15\%$, 20%, and 53% InGaAs composition are all within 0.7% range and better in some cases. The longest data span covers a period of 5 months.

© 2002 Elsevier Science B.V. All rights reserved.

PACS: 81.15.Hi; 81.70.Fy; 85.30.Pq; 85.30.Tv

Keywords: A3. In situ sensors; A3. Molecular beam epitaxy; A3. Real-time growth monitor; B2. Semiconducting gallium arsenide; B2. Semiconducting indium phosphide; B3. Heterojunction semiconductor devices

1. Introduction

For some of the high-performance electronic devices such as GaAs-based PHEMTs and InP-based HBTs, epi-materials grown by MBE have emerged as the preferred choice. Compared to MOCVD, MBE offers the distinct advantage of abrupt heterointerfaces, especially for layers such as InGaAs channels in PHEMTs. Furthermore, for InP-based HBTs, the InGaAs base can be highly p-doped with CBr_4 well into the mid $10^{19}\,cm^{-3}$ without any p-type doping diffusion related issues. To remain commercially viable, it also requires that the epi-growth can be constantly maintained within the required growth process window to minimize non-productive runs. From a production perspective, an out of specification run lowers the yield and adds to the cost. This becomes even more critical as the MBE reactor scales up in size and utilizes more expensive substrates such as InP. By deploying robust in situ sensor technologies such as atomic absorption optical-based flux

*Corresponding author. Tel.: +1-9722340068x102; fax: +1-9722340069.

E-mail address: pinsu@intelliepi.com (P.R. Pinsukanjana).

0022-0248/03/$ - see front matter © 2002 Elsevier Science B.V. All rights reserved.
doi:10.1016/S0022-0248(02)02293-5

monitor (OFM) for the group III elements and absorption band edge spectroscopy for accurate substrate temperature measurement during each growth layer, the ability to quantify and maintain MBE growth conditions will improve significantly.

Optical atomic absorption spectroscopy has long been recognized as a versatile and sensitive monitor of molecular beam flux [1]. However, its use has mostly been confined to research and development efforts [1–11]. In this work, we present the use of OFM in a commercial production MBE environment. With our multi-channel OFM implementation, we monitor the molecular beam fluxes of the group III elements namely Al, Ga, and In simultaneously in real time. Absorption flux profile taken during each growth run is also used for growth layer verification. Furthermore, we compare the use of OFM for InGaAs composition measurement to X-ray diffraction and quantify the reliability of the data set taken over the span of several months.

2. OFM setup

The optical design of our OFM is similar to previous work [8–11], but with the addition of a blue LED channel for optical transmission path correction. A schematic of the optical setup is shown in Fig. 1. The atomic emission lines from three hollow cathode lamps (HCL) are combined along with the calibration blue LED [11] into a single optical fiber network. Each HCL is operated under constant current mode. Light from each lamp is modulated via a mechanical chopper, and the blue LED is modulated electronically. A small portion of the combined beam is split off to the reference detector, and the rest is collected into the probe fiber. The probe fiber guides the light into the growth chamber where it is passed through the molecular beams just in front of the substrate platen, reflected back by a pair of mirrors, and collected with another collection fiber directing it to the signal detector. The reference and the signal detectors are both photomultiplier tubes. This dual pass configuration nearly doubles the measured absorption for a given growth rate. Optical access is provided by a pair of heated viewports to reduce signal drift caused by As coating. All the data acquisition and lock-in signal recovery are processed directly through a personal computer.

In our implementation, the optical beam path is positioned away from the substrate platen; therefore, OFM measurement is not affected by substrate wobbling during platen rotation. It is possible to overcome the wobble limitations by having a specially designed substrate manipulator for in situ ellipsometry, or to rotate the substrate manipulator extremely fast for synchronous RHEED oscillation [12]. However, these options add extra burden on the MBE operation, and/or cause unnecessary wear and tear to the MBE system. This makes them impractical to implement in a production environment. Furthermore, for

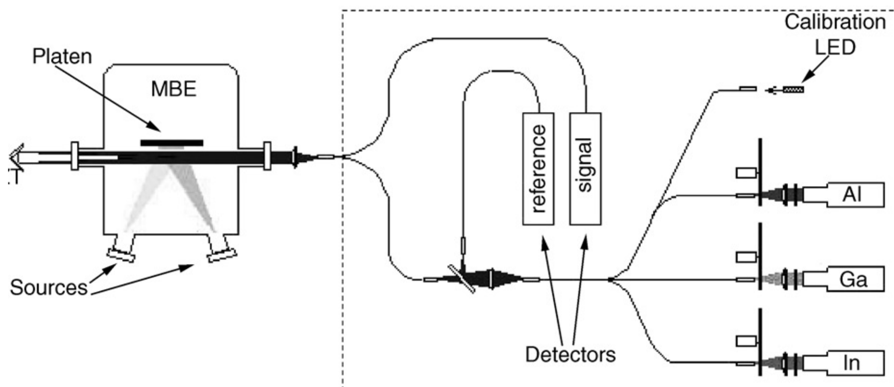

Fig. 1. Schematic diagram of atomic absorption flux monitor setup. The components inside the dashed box are mounted on a small optical breadboard. Optical fibers transmit and collect light that passes through the molecular beams.

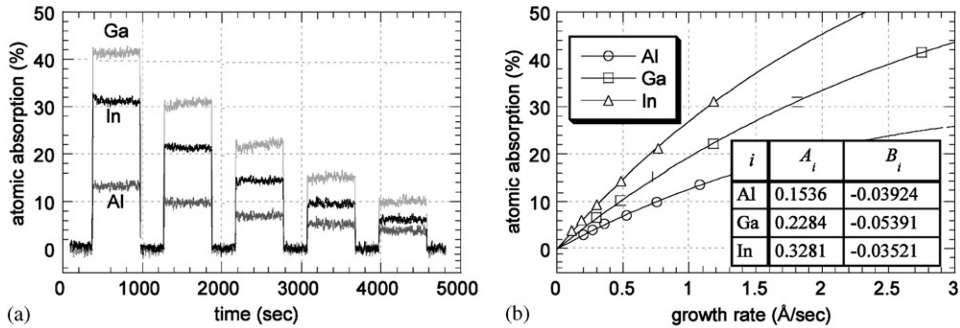

Fig. 2. (a) Atomic absorption profile of a Riber 6000 (4×6 in) taken during a series of programmed cell temperature steps from high to low. (b) OFM absorption vs. growth rate for each of the cell temperature steps. Curves through the data are modified Beer's law fits according to Eq. (1). Inset table lists the fit coefficients.

multi-wafer production MBE reactors, the issues of which spot on which wafer to probe also becomes a concern. As an in situ optical measurement technique, OFM also has the advantage of being non-invasive to the growth process.

Because the measured optical atomic absorption line for each of the atomic species is at a distinct wavelength, the group III beam fluxes during MBE growth, namely Al, Ga, and In, can be measured simultaneously. The atomic absorption intensity for each of the atomic species being monitored is directly related to the concentration of the atomic vapor that crosses path with the optical probe beam. Under typical MBE growth condition where the group III fluxes have unity sticking coefficients or very close to it, there is a direct correspondence between atomic absorption strength and growth rate for each of the species.

To calibrate OFM absorption to the growth rate, we look at the changes in the atomic absorption flux profile at different group III cell conditions. Fig. 2a shows the three overlaying atomic absorption profiles vs. time during a programmed cell temperature calibration for Al, Ga, and In cells. Between each set of temperature steps, a 5 min interruption is used for cell stabilization. Fig. 2b compares the atomic absorption signal levels for each cell to their corresponding growth rates. The data for each material can be fitted quite well with a modified Beer's law of the form

$$\mathrm{abs}_i = 1 - \exp\left[-A_i r_i (1 + B_i r_i)\right], \qquad (1)$$

where abs_i is the atomic absorption for material i, r_i is growth rate, and A_i, B_i are the fit coefficients [8]. For this plot, the growth rates at the selected cell temperatures were taken from an already existing calibration table. Other in situ cross calibration methods include the use of other in situ measurements such as RHEED oscillation, laser reflection interferometry, pyrometric interferometry, or white light reflection. These techniques typically work well for material systems nearly lattice matched to the substrate, such as GaAs or AlAs on GaAs substrate.

3. Flux profile during epi-growth

The Al, Ga, and In OFM absorption profiles during each run become a record of the growth process. Figs. 3a–d show profiles from epi-structures lattice matched to InP-, and GaAs-based PHEMT. The absorption data are collected once every 0.1 s. This time resolution is sufficient for verification of the shutter actions under normal growth conditions. Fig. 3a is an HBT with a single heterojunction grown on InP; and Fig. 3b, an InGaAs layer lattice matched to InP. Figs. 3c and d are GaAs-PHEMTs with InGaAs channels. For Fig. 3d, the second layer with In and Ga absorptions to the right of the channel corresponds to an InGaP etch-stop for a gate recess etch.

As seen in Fig. 3, the absorption profiles from Riber 6000 (Figs. 3b and d) show almost twice the

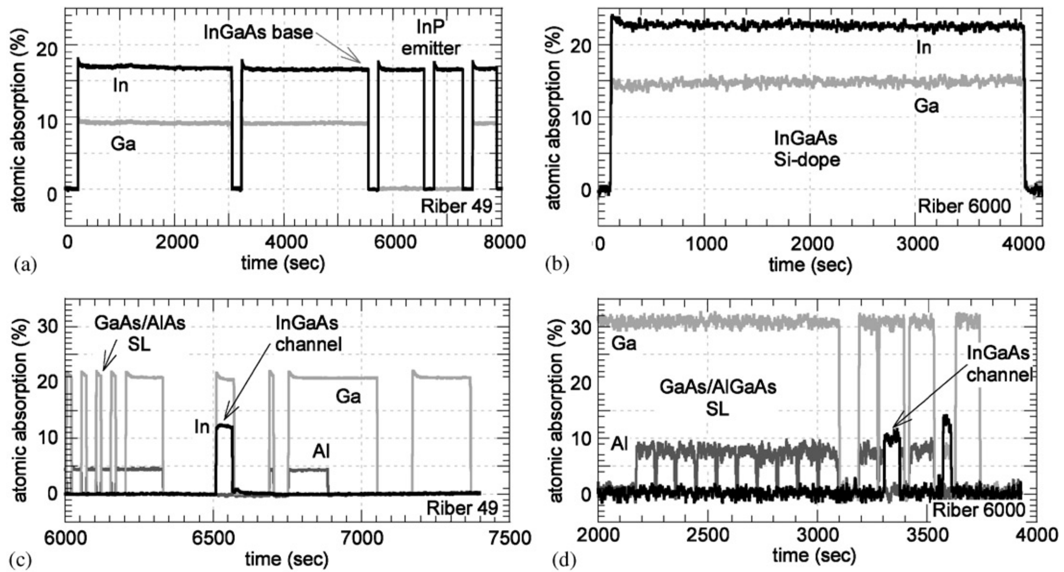

Fig. 3. Atomic absorption profiles from actual growth runs. (a) InP-based HBT consisting of InP and InGaAs layers. (b) Si–InGaAs lattice matched to InP. Growth rate (∼2 Å/s) is similar to (a). (c) and (d) are GaAs-based PHEMTs. GaAs growth rate ∼2 Å/s.

absorption strength compared to their counterparts with the same target growth rate when grown by a 4×4 in Riber 49 (Figs. 3a and c). Fig. 4 shows a comparison of the absorption strength for a Riber 6000 (4×6 in) for comparable Ga and In growth rates. The stronger absorption strength is due to the larger reactor size. To maintain the same growth rate and uniformity across a larger platen size requires more molecular beam coverage. This translates to an increased cross sectional overlap between the OFM optical probe beam and the molecular beams during the MBE growth for the larger reactor.

In terms of measurement noise, the observed signal to noise varies depending on the exact optical setup and the background light pollution from each system. Compensation for baseline drift due to viewport coating is calculated from the non-absorbing blue LED light that shares the optical path. The non-absorbing baseline reference level for each material species is assumed to be proportional to the blue LED signal raised to a specified power. Other possible sources of error include the change in the HCL optical emission line shape, the change of the molecular flux profile as the group III source materials change shape,

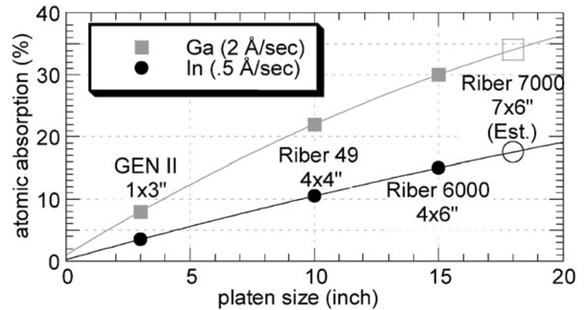

Fig. 4. Scaling of atomic absorption strengths with size of MBE reactor. This graph compares Ga and In absorption vs. platen diameter for $In_{0.2}Ga_{0.8}As$ for Ga and In growth rates of 2 and 0.5 Å/s, respectively. Data at each platen diameter is labeled with reactor type and a representative platen configuration. Data for GEN II came from Ref. [8]. Data for Riber 7000 is estimated.

and the mechanical vibrations or movements from the MBE reactor.

4. InGaAs composition measurement by OFM

With the availability of both In and Ga flux profiles from OFM, the indium composition for layers such as the strained InGaAs channel in a

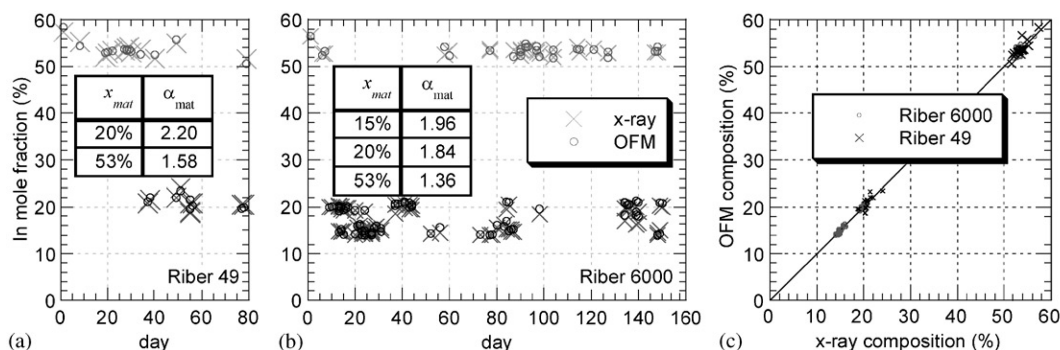

Fig. 5. (a) and (b) Charts of InGaAs compositions measured by OFM and post-growth X-ray diffraction vs. time. The open circles are data from OFM; and x's from X-ray. The strips of data around 53% indium mole fraction are from growths with InGaAs lattice matched to InP. The data in the 15–20% ranges are from PHEMT channels. The two data sets span periods of 80 and 150 days, respectively. α_{mat}'s are given in each inset. (c) Comparison of OFM to X-ray InGaAs composition from (a) and (b). The diagonal line is reference if two methods are equal.

GaAs PHEMT, or an InGaAs layer lattice matched to InP in an HBT can be measured in situ. The following expression is a simple approach that we take to calculate indium mole fraction from OFM absorption data:

$$x_{mat} = \frac{abs_{In}}{abs_{In} + \alpha_{mat} abs_{Ga}}. \quad (2)$$

In this equation, x_{mat} is the indium mole fraction for each material system mat; abs_{In} and abs_{Ga} are the corresponding atomic absorption measurements; and α_{mat} is the material-system specific tooling factor. For each material system, α_{mat} is roughly the ratio of the atomic absorption strength of Ga to In at their respective growth rates. α_{mat} is obtained by taking the average of the back calculated α_{mat} values for all the runs within a calibration set. Composition data from X-ray diffraction is used as reference for the back calculations. Figs. 5a and b show the InGaAs composition data obtained from X-ray diffraction and OFM plotted over time. For the data shown, a single α_{mat} for each of the three material systems was used—one for the 53% InGaAs lattice matched to InP, and one each for 15% and 20% ranges for strained InGaAs channel in PHEMTs. The alpha value for each material system is fixed for this analysis work. Fig. 5c replots the same data as OFM composition vs. X-ray. The better the agreement is, the less the scatter from the line.

Table 1
Standard deviation of the difference between OFM and X-ray InGaAs composition

Composition range	15%	20%	53%
Riber 49		±0.7%	±0.7%
Riber 6000	±0.3%	±0.3%	±0.7%

The spread is calculated from the data in Fig. 5. The units are in indium mole fraction (%).

The discrepancies between OFM and X-ray for the different material systems and reactors are summarized in Table 1. In the worst case, the OFM InGaAs composition agrees with X-ray to within a standard deviation of 0.7 at%. Some of the possible sources of discrepancies between the two measurements are (a) noise from the OFM absorption signals—this can come from the noise level with respect to the signal and the possible drift of the no-absorption reference baseline, (b) the accuracy of the simulation to the X-ray diffraction spectra, (c) change in the group III cell beam distribution profiles, and (d) the non-unity sticking coefficients of the group III materials under deviation from standard growth conditions.

5. Conclusion

We have established an atomic absorption measurement technique as a practical in situ tool

for simultaneous monitoring of the group III molecular beam fluxes within a production MBE environment. With OFM, a direct method for confirming group III flux profiles during each layer growth is now available. Through implementations on several sizes of multi-wafer MBE reactors, we confirmed that the absorption strength for comparable growth rates become stronger with larger platen diameter size due to increased molecular beam cross sections. As a tool for InGaAs composition monitoring, a correlation between OFM and X-ray measurements at least at the ± 0.7 level of indium mole fraction percentage during a period of 5 months has been demonstrated. Better agreement at ± 0.3 level with a 4×6 in reactor has been observed for the composition ranges of 15 and 20 indium mole fraction percentage. While OFM is not the only way to obtain the critical growth parameters such as growth rate and ternary materials composition, it is one of the few techniques that offer detailed and immediate information during growth. Furthermore, this technique is non-invasive to the growth process, and is not plagued by issues related to multi-wafer platen rotation.

Acknowledgements

The authors would like to thank K. Vargason, J.R. Thomason, X.-J. Jin, and the production staff at IntelliEPI for their support. We would also like to thank J.-M. Kuo for insightful discussions.

References

[1] T.Y. Kometani, W. Wiegmann, J. Vac. Sci. Technol. 12 (1975) 933.
[2] M.E. Klausmeier-Brown, J.N. Eckstein, I. Bozovic, G.F. Virshup, Appl. Phys. Lett. 60 (1992) 657.
[3] S.A. Chalmers, K.P. Killeen, Appl. Phys. Lett. 63 (1993) 3131.
[4] S.A. Chalmers, K.P. Killeen, E.D. Jones, Appl. Phys. Lett. 65 (1994) 4.
[5] S.J. Benerofe, C.H. Ahn, M.M. Wang, K.E. Kihlstrom, K.B. Do, S.B. Arnason, M.M. Fejer, T.H. Geballe, M.R. Beasley, R.H. Hammond, J. Vac. Sci. Technol. B 12 (1994) 1217.
[6] C. Lu, Y. Guan, J. Vac. Sci. Technol. A 13 (1995) 1797.
[7] P.D. Brewer, K.P. Killeen, Diagnostic Techniques for Semiconductor Materials Processing, Vol. II, Boston, MA, 1995.
[8] P. Pinsukanjana, A. Jackson, J. Tofte, K. Maranowski, S. Campbell, J. English, S. Chalmers, L. Coldren, A. Gossard, J. Vac. Sci. Technol. B 14 (1996) 2147.
[9] A.W. Jackson, P. Pinsukanjana, L. Coldren, A. Gossard, J. Crystal Growth 175/176 (1997) 244.
[10] A.W. Jackson, P.R. Pinsukanjana, A.C. Gossard, L.A. Coldren, IEEE J. Select. Topics Quantum Electron. 3 (1997) 836.
[11] A.W. Jackson, P.R. Pinsukanjana, A.C. Gossard, L.A. Coldren, J. Crystal Growth 201/202 (1999) 17.
[12] J.P.A. van der Wagt, J.S. Harris Jr., J. Vac. Sci. Technol. B 12 (1996) 1236.